

# Tuning Polydimethylsiloxane (PDMS) properties for biomedical applications

Etienne Mfoumou<sup>1\*,2</sup>, Martin Tango<sup>2</sup>, Pak Kin Wong<sup>3</sup>

<sup>1</sup>Applied Research & Innovation, Nova Scotia Community College, Ivany Campus, Dartmouth, NS, B2Y 0A5, Canada

<sup>2</sup>Ivan Curry School of Engineering, Acadia University, Wolfville, NS, B4P 2R6, Canada

<sup>3</sup>PennState College of Engineering, Pennsylvania State University, University Park, PA 16802, USA

\*Corresponding author: Tel: (+1) 902 491 1692; E-mail: etienne.mfoumou@nsc.ca

DOI: 10.5185/amlett.2019.2130

www.vbripress.com/aml

## Abstract

Polydimethylsiloxane (PDMS) is used extensively to study cell-substrate interactions because its mechanical properties are easily tuned in physiologically relevant ranges. These changes in mechanical properties are also known to modulate surface chemistry and cell response. In this study, PDMS pre-polymer was combined with increasing amounts of cross-linker (3.3, 5.0, 10.0, 12.5, 20.0 and 33.3 wt.%). The solutions were mixed in sterile conditions and degassed, then poured into 60 mm cell culture dishes to a depth of 1 mm. This was followed by curing at a constant temperature of 75 °C for 2 hours. The PDMS substrates were then exposed to an air plasma for 10 minutes. All substrates were exposed to UV light for further sterilization and understanding of the structure/morphology of the substrates was obtained with microscopic techniques. A SH-SY5Y neuroblastoma cell line was used in cell culture experiment. Cells were plated at a concentration of  $300 \times 10^6$  cells/dish on plasma treated PDMS substrates and incubated at 37 °C in a humidified 5 % CO<sub>2</sub> environment. For the assessment of morphological changes, images of cells growing on each substrate were captured using an inverted phase contrast microscope. Cell adhesion as well as immunofluorescence analyses were conducted, and the mechanical as well as surface properties of PDMS were correlated to neuroblastoma cell behaviour. The results reveal that the physicality of the extracellular matrix/environment (ECM) substrate governs cell behavior regardless of hormones, cytokines, or other soluble regulatory factors. The approach used in this study may open up new avenues in translational medicine and pharmacodynamics research. Copyright © 2019 VBRI Press.

**Keywords:** Polydimethylsiloxane, cell-substrate interactions, cell culture, cell transdifferentiation, mechanical and surface properties.

## Introduction

In the neurosciences, many questions exist that center on how Extra Cellular Matrix (ECM) affects synaptic and cellular structure. In culture, it is generally believed that using stiffer PDMS substrate leads to a better cell viability [1-3], still the optimum stiffness is currently undefined. In recent years, it has become desirable and conceptually feasible to study the effects of substrate stiffness on cells in vitro [4, 5]. From these studies has emerged an improved understanding of cell culture on different substrate rigidities. Yet a major need still exists for better control of the precise spatial development and geometric interaction of neural cells, both for fundamental studies in vitro and for a variety of focused applications, such as evaluation of pharmaceuticals and development of biosensors. With such cultures, it should be possible to determine the type of parameters of change as a function of ECM rigidity and to monitor not only mechanical activity but also metabolic and structural change of neurons.

Many established neuroblastoma cell lines possess at least three morphological variants contributing to the

heterogeneity in these cell lines: the neuroblastic (N), flat or substrate adherent (S) and intermediate (I) cell types [6-8]. A study of cell surface antigen expression indicated that the S-type cells shared antigenic characteristics more in common with a fibroblast-like meningeal cell rather than a Schwannian cell [8]. Meanwhile, neural crest cells can give rise to ectomesenchyme, including skeletal and connective tissues of the head and face which also includes meninges. These features have led to a model in which N-type cells are proposed to resemble embryonic sympathoblasts, S-type cells resemble Schwannian, glial or melanocytic progenitor cells or ectomesenchymal derivatives and the I-type cells have an intermediate phenotype and the potential to differentiate to N- or S-type cells [7].

PDMS has been a long-serving material for manufacturing systems in biomedical applications as it is biocompatible, robust, cost-effective and simple to handle and is also considered well suited for the development of lab-on-a-chip devices [9, 10]. Depending on its Young's modulus or stiffness, PDMS may be assigned to one of the three types S-, H-, and

X-PDMS, which are differently amenable to generating nano- to micrometer-patterned matrices and thus, mimicking the three-dimensional topography of the native ECM. Soft or S PDMS, the most commonly used type is used in this study and has proven useful for a variety of biomedical applications, including tissue engineering and microfluidics systems. The study is a contribution to the existing body of knowledge in the field and focuses on developing a basic understanding of the relationships between the developmental morphologies of cultured neurons and the quantitated mechanical characteristics of the substrates. Progress toward a quantitative understanding of the role of the substrate is crucial not only to neuronal patterning but also to the interpretation of experiments involving regulators of cell metabolism *in vitro* and future applications requiring the rational design of neuronal substrates.

## Experimental

### Preparation of PDMS substrate for experiments

The PDMS used in this work is a liquid bi-component silicone pre-polymer, Sylgard 184 manufactured by Dow Corning (Midland, MI). The substrate stiffness can be controlled by the base (pre-polymer) to hardener (curing agent) ratio, determining the cross-linker agent concentration in the PDMS solution. Other key parameters for manipulating this mechanical property are temperature and curing time. As the time and curing temperature are closely linked, we chose to cure the PDMS substrates at a constant temperature of 75 °C for 2 hours. The solutions were mixed in sterile conditions and degassed, then poured into 24 well plates to a depth of about 1 mm. The mixed and degassed solutions were cured at 75 °C for 2 hours. The “untreated” dishes with PDMS substrates were rinsed three times in sterile PBS, then once in 100 % ethanol during two minutes, and air dried in sterile conditions. The “treated” dishes with PDMS substrates were exposed to air plasma for 10 minutes at 29.6 W using a plasma machine (Harrick, model PDC-001), with air entering the chamber at 150 Pa. All plates were then exposed to UV light in the biological safety cabinet for further sterilization, from a transilluminator for 20 minutes from a distance of 30 cm.

### Substrate characterization

For the measurement of the stiffness of the fabricated substrates, we used a Digital Instruments Nanoscope III Multimode to indent the sample with an Atomic Force Microscope (AFM) tip, a three-sided pyramid blunt indenter mounted on a stiff steel cantilever. The nanoindentation test consisted of applying a load ( $F$ ) on the indenter and subsequently removing the load. According to the procedure described by Cappella *et al.* [11], the AFM piezoelement was ramped up until the contact between the sample and the tip was observed. From this point, a further piezo displacement  $z$  provoked the cantilever to bend of a quantity  $\delta$  thus applying a load:

$$F = k\delta \quad (1)$$

Where,  $k$  is the normal elastic constant of the cantilever.

The nanoindentation then took place while the cantilever bends and resulted in a penetration depth given by:

$$p = z - \delta \quad (2)$$

The piezo displacement  $z$  and the cantilever deflection  $\delta$  were then recorded in order to obtain a common  $F$  vs.  $p$  force curve from equations (1) and (2), from which the stiffness of the substrate was estimated.

### Cell line and low density culture conditions

The SH-SY5Y cell line used is a thrice cloned subline of SK-N-SH cells which were originally established from a bone marrow biopsy of a neuroblastoma patient with sympathetic adrenergic ganglia origin in the early 1970's [12]. Using current culture technology, neurons are usually randomly organized, and their dendrites and axons overlap. This makes geometrically dependent studies of minor processes in neuron's development extremely difficult, if not impossible. Therefore, we have adopted a low density culture for two reasons: (i) it allows driving and monitoring neuronal growth in response to PDMS substrate stiffness changes; (ii) it allows correlating the dynamic changes of the cell activity with its topology and PDMS substrate mechanical properties.

The culture medium used was a 1:1 mixture of Eagle's minimum essential medium with nonessential amino acids and Ham's nutrient mixture F-12, supplemented with 15% heat-inactivated fetal bovine serum and 1% penicillin-streptomycin. Derived from immature neoplastic neural crest cells that exhibit properties of stem cells, SH-SY5Y were induced to differentiate upon treatment with retinoic acid (RA) [13].

### Cell proliferation and morphological change measurements

Cells were plated at  $300 \times 10^6$  cells/well on plasma treated PDMS substrates. For the assessment of morphological changes, images of cells growing on each substrate were captured using an inverted phase contrast microscope equipped with a controller software. Eight to ten distinct snapshots of representative areas of each well were examined with the freeware ImageJ software (available at <http://rsb.info.nih.gov/ij>). Single cells were identified by their boundaries and the approximate perimeter measured by tracing the border of five cells per image and using the “Perimeter” function in ImageJ.

For adhesion analysis, 20 and 60 hours incubated cells were washed twice in PBS, fixed for 15 minutes with 70 % (v/v) ethanol to preserve the shape as much as possible, and washed again twice in PBS. After fixation, cells were stained with 0.5% (w/v) crystal violet for 10 minutes and dye was extracted from cells with 0.1 M citric acid. Absorbance was measured at 590 nm on an absorbance spectrometer.

### Immunofluorescence and adhesion measurements

Cells were stained for F-actin with Alexa Fluor 555 tagged phalloidin (Invitrogen), for nuclei with ProLong Gold antifade reagent with 4', 6-diamidino-2-phenylindole (DAPI) (Invitrogen), and for vinculin to mark focal adhesions with monoclonal anti-vinculin-FITC antibodies (Sigma-Aldrich). The cells, on PDMS substrate, were first fixed with 3.7% formaldehyde (Polysciences Inc.), and permeabilized with 0.1% Triton X-100 (Astoria-Pacific). Then, they were stained and the antifade reagent was added before cover slips were placed over the cells and sealed with nail polish.

### Results and discussion

The difference in PDMS substrate stiffness rendered by the variation of the cross-linker concentration is shown in **Fig. 1**. The stiffness values increase, reaches a maximum, then decreases within the cross-linker concentration analyzed (from 3.33 to 33.33 %). This trend is comparable to the one obtained by Evans *et al.* [14], who measured the Young's modulus of PDMS at cross-linker concentrations varying from 1 to 23%. This technique is a versatile and easy to implement *in vitro* method of inducing mechanotransduction on cells, for which the exchange with the extracellular environment (here the culture medium) can be noninvasively characterized with spectrophotometry of a small volume of culture medium.

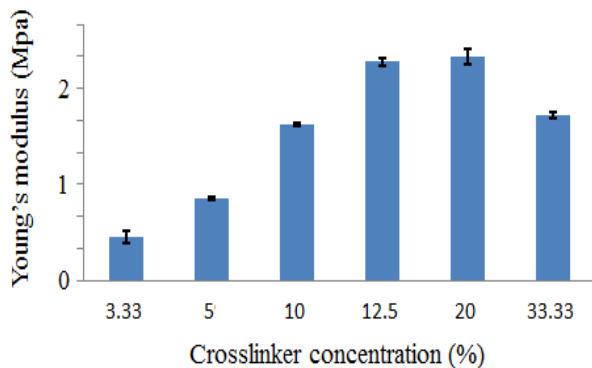


**Fig. 1.** The Young's modulus of PDMS with crosslinker concentration varying from 3.3 to 33.3%. The values and error bars represent the mean and standard deviation of ten measurements on each sample.

**Fig. 2** shows representative fluorescence images of RA-differentiated SH-SY5Y cultured on PDMS with 3.33 %, 12.5 %, and 33.3 % crosslinker concentrations. Cells were stained with antivinculin antibodies to mark focal adhesions (Green) and DAPI for nuclei labelling (Blue). The figure also illustrates the approach used for counting focal adhesion points. A white square in each panel represents a region of interest on a neurite. A zoomed view of the corresponding regions of interest is reported as inset in the upper right corner of each panel. White arrowheads in the inset point to the visible focal adhesions.

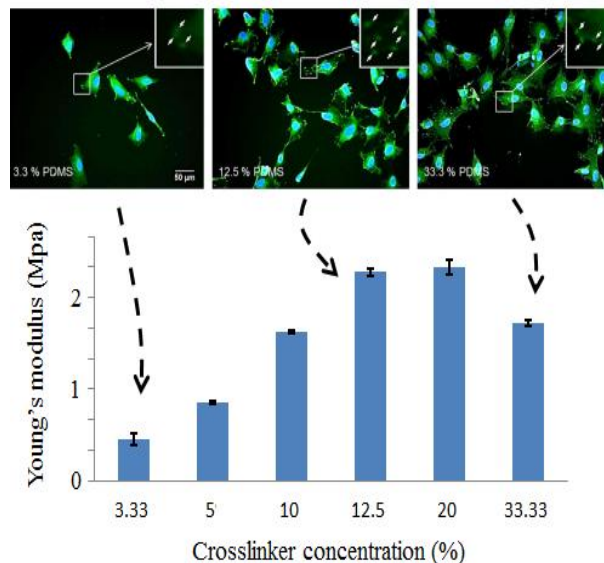


**Fig. 2.** Representative fluorescence images of RA-differentiated SH-SY5Y on day #8, cultured on PDMS with 3.33 % (left), 12.5 % (middle), and 33.3 % (right) crosslinker concentrations.

Evidences of the effect of substrate stiffness on cell adhesion and differentiation are shown in **Figs. 3 to 6** below. **Fig. 3** shows the average measured length of neurites on different substrate rigidities on day #8 in culture. 96 cells from three experiments were analyzed for the calculations in each group. The average neurite length is shown to decrease with an increase in the substrate rigidity. Error bars represent the measured standard deviation in each set of data.

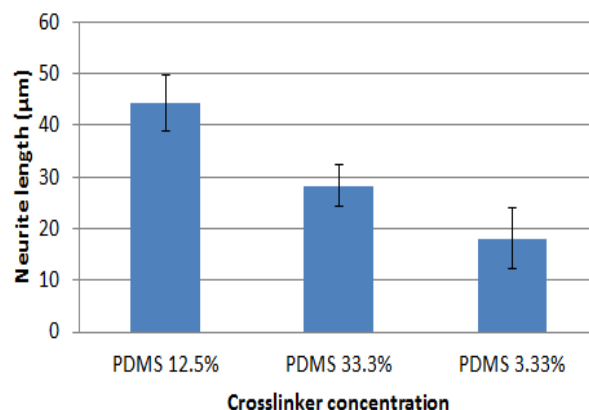


**Fig. 3.** Average measured length of neurites on different substrate rigidities after 9 days in culture. A total of 96 cells from three experiments were analyzed for the calculations in each group. The average neurite length decreases with an increase of the substrate rigidity. Error bars represent the measured standard deviation in each set of data.

**Fig. 4** presents the average number of focal adhesions on substrates of different rigidity. 40 cells from three experiments were analyzed for the calculations in each group and the average neurite length decreases with an increase in the substrate rigidity. Error bars represent the measured standard deviation in each set of data.

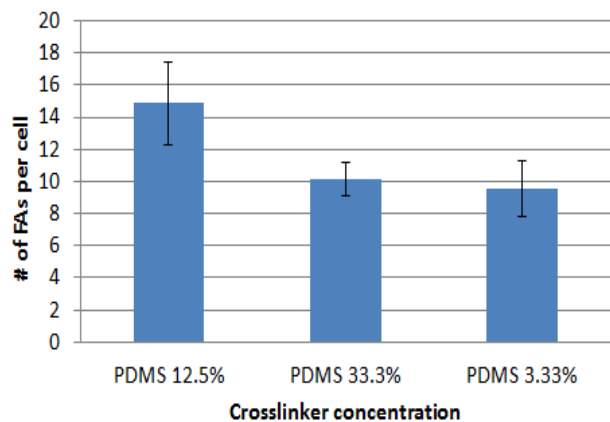


**Fig. 4.** Average number of focal adhesions on substrates of different rigidity. A total of 40 cells from three experiments were analyzed for the calculations in each group. The average neurite length decreases with an increase of the substrate rigidity. Error bars represent the measured standard deviation in each set of data.

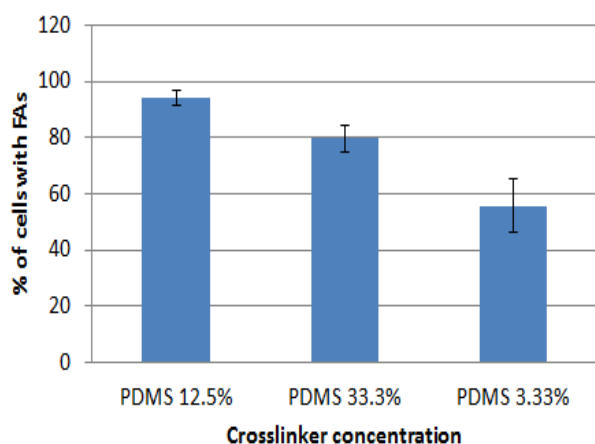


**Fig. 5.** Average percentage of cells with responsive Focal Adhesion Kinase (FAK). A responsive cell was defined as a cell having at least three focal adhesion points. A total of 40 cells from three experiments were analyzed for the calculations in each group and the number of responsive cells decreases with an increase in the substrate rigidity. Error bars represent the measured standard deviation in each set of data.

**Fig. 5** presents the average percentage of cells with responsive Focal Adhesion Kinase (FAK). A responsive cell was defined as a cell having at least three focal adhesion points. Here again, 40 cells from three experiments were analyzed for the calculations in each group and the number of responsive cells decreases with an increase in the substrate rigidity. Error bars represent the measured standard deviation in each set of data.

Finally,

**Fig. 6** shows a classification of focal adhesions by size and by group. Focal adhesion sizes were defined as small (less than  $2 \mu\text{m}^2$ ), medium (between 2 and  $4 \mu\text{m}^2$ ), and large (more than  $4 \mu\text{m}^2$ ). An amount of 680 focal adhesions were analyzed and we observe a predominance of large focal adhesions in all cases, with the larger of the stiffer substrate (PDMS 12.5 %).

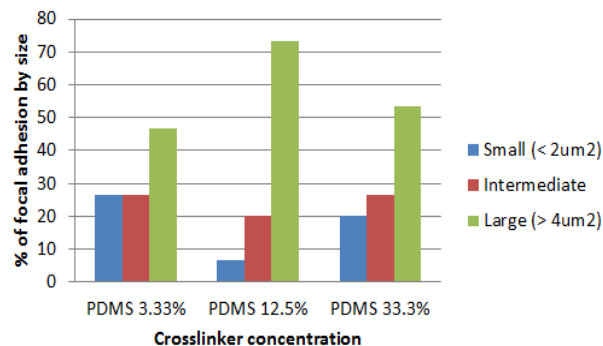


**Fig. 6.** Focal adhesion by size and group. Defined as small (less than  $2 \mu\text{m}^2$ ), medium (between 2 and  $4 \mu\text{m}^2$ ), and large (more than  $4 \mu\text{m}^2$ ). A total of 680 focal adhesions were analyzed.

These observations are in good agreement with the results reported by Lo *et al.* [15] on fibroblasts. Nonetheless, the plasma lithography patterning on PDMS substrates for elucidating the influences of mechanical cues on neuronal differentiation and neurogenesis has been reported by Nam *et al.* [16]. In that study, systematic adjustment of these cues, along with computational biomechanical analysis demonstrated the interrelated mechanoregulatory effects of substrate elasticity and cell size. These findings reveal that the neuronal differentiations of neuroblastoma cells are collectively regulated via the cell-substrate mechanical interactions.

## Conclusion

This work shows that modifying PDMS cross-linker concentration to tune substrate rigidity plays a role in neuroblastoma adhesiveness and development of axonal/dendritic polarity. A correlation between higher PDMS surface energy (hydrophilicity), higher cell adhesion, higher cell surface, and larger cell polarization has been found. Indeed, an increase in the substrate's stiffness highly favors cell adhesion, which is correlated with significantly more polarized cells. Moreover, stiffer substrates promote significantly faster neurite extension than softer ones, and there is a high compliance of undifferentiated cell proliferation rate with substrate's stiffness variation. Thus, the results show that adequate tuning of the substrate mechanical properties and surface's physical chemistry can control the neuroblastoma cells adhesion and morphology, opening up new avenues in translational medicine and pharmacodynamics research.

## Acknowledgements

This work was supported by National Institutes of Health Director's New Innovator Award (DP2OD007161) for cell culture and cell-substrate interactions analysis, and the Nova Scotia Community College.

## Author's contributions

Conceived the plan: EM, PKW; Performed the experiments: EM; Data analysis: EM, PKW, MT; Wrote the paper: EM, MT. Authors have no competing financial interests.

## References

1. Yeh, Y.; Corbin, E.A.; Caliari, S.R.; Ouyang, L.; Vegaa, S. L.; Truitt, R.; Han, L.; Margulies, Kenneth B.; Burdick, Jason A., *Biomaterials*, **2017**, *145*, 23.  
**DOI:** 10.1016/j.biomaterials.2017.08.033
2. Voiculescu, I.; Li, F.; Liu, F.; Zhang, X., Cancel, Limary M.; Tarbell, John M.; Khademhosseini, A.; *Sensors and Actuators B*, **2013**, *182*, 696.  
**DOI:** 10.1016/j.snb.2013.03.030
3. Park, J.Y.; Yoo, S.J.; Lee, E.J.; Lee, D.H., Kim, J. Y.; Lee, Sang-Hoon, *BioChip J.*, **2010**, *4*, 230.  
**DOI:** 10.1007/s13206-010-4311-9
4. Wu, H.M.; Lee, T.A.; Ko, P.L.; Chiang, H.J., et al.; *J. Micromechanics Microengineering*, **2018**, *28*, 230.  
**ISSN:** 0960-1317
5. Scharin-Mehlmann, M.; Haring, A.; Rommel, M.; Dirnecker, T., et al.; *Front. Bioeng. Biotechnol.*, **2018**, *6*, 51.  
**DOI:** 10.3389/fbioe.2018.00051
6. Ross, R.; Domenech, B.; Porubcin, C.; Rettig, M., et al.; *Cell Growth Differ.*, **1995**, *6*, 449.  
**ISSN:** 1044-9523
7. Ross, R.; Spengler, B.A.; Rettig, W.J.; Biedler, J.L., *Prog. Clin. Biol. Res.*, **1994**, *385*, 253.  
**ISSN:** 0361-7742
8. Biedler, J.L.; Helson, L.; Spengler, B.A., *Cancer Res.*, **1973**, *33*, 2643.  
**ISSN:** 0008-5472
9. Halldorsson, S.; Lucumi, E.; Gomez-Sjoberg, R.; Fleming, RMT., *Biosens. Bioelectron.*, **2015**, *63*, 218.  
**DOI:** 10.1016/j.bios.2014.07.029
10. Zhou, J.; Khodakov, D.A.; Ellis, A.V; Voelcker, N.H; *Electrophoresis*, **2012**, *33*, 89.  
**DOI:** 10.1002/elps.201100482
11. Cappella, B.; Dietlet, G., *Surf. Sci. Rep.*, **1999**, *34*, 1.  
**DOI:** 10.1016/S0167(99)00003-5
12. Singh, J.; Kaur, G., *Brain Res.*, **2007**, *1154*, 8.  
**DOI:** 10.1016/j.brainres.2007.04.015
13. Fagerstrom, S.; Pahlman, S.; Gestblom, C.; Nanberg, E.; *Cell Growth Differ.*, **1996**, *7*, 775.  
**PMID:** 8780891
14. Evans, N.D.; Minelli, C; Gentleman, E., et al.; *Eur. Cell. Mater.*, **2009**, *18*, 1.  
**PMID:** 19768669
15. Lo, C.M.; Wang, H.B.; Dembo, M.; Wang, Y.I., *Biophys. J.*, **2000**, *79*, 144.  
**DOI:** 10.1016/S0006-3495(00)76279-5
16. Nam, K.H; Jamilpour, N.; Mfoumou, E.; Wang, F.Y., et al.; *Sci. Rep.*, **2014**, *4*, 6965.  
**DOI:** 10.1038/srep06965